Optics & Laser Technology 52 (2013) 30–36

Contents lists available at SciVerse ScienceDirect

Optics & Laser Technology

journal homepage: www.elsevier.com/locate/optlastec

Carbide and nitride precipitation during laser cladding of Inconel 718 alloy coatings

Yaocheng Zhang [a], Zhuguo Li [a,*], Pulin Nie [a], Yixiong Wu [a,b]

[a] Shanghai Key Laboratory of Materials Laser Processing and Modification, School of Materials Science and Engineering, Shanghai Jiao Tong University, Shanghai 200240, China

[b] State Key Laboratory of Metal Matrix Composites, School of Materials Science and Engineering, Shanghai Jiao Tong University, Shanghai 200240, China

ARTICLE INFO

Article history:
Received 11 January 2013
Received in revised form
13 March 2013
Accepted 29 March 2013
Available online 3 May 2013

Keywords:
Inconel 718
Laser clad
Precipitation

ABSTRACT

The microstructure of the laser clad Inconel 718 alloy coating was observed by scanning electron microscope (SEM). The chemical composition of precipitation phases was investigated by energy dispersive spectrometer (EDS) and solid phase microextraction (SPME). The crystal structure and lattice constants of precipitation are determined by transmission electron microscope (TEM). Vickers hardness of the coatings and the nanohardness of the interstitial phases were measured. The insular carbide (MC) and the tetragonal nitride (MN) with face-centered cubic (FCC) structure are rich in Ti and Nb but depleted in Ni, Fe and Cr due to the interdiffusion and redistribution of alloying elements between MC and MN and supersaturated matrix. MC and MN were precipitated in the forms of $(Nb_{0.12}Ti_{0.88})C_{1.5}$ and $(Nb_{0.88}Ti_{0.12})N_{1.5}$, and the Gibbs free energies of formation can be expressed as $\Delta G^0_{[(Nb_{0.12}Ti_{0.88})C_{1.5}]} = -122.654–3.1332\ T$(kJ/mol) and $\Delta G^0_{[(Nb_{0.88}Ti_{0.12})N_{1.5}]} = -157.814–3.0251\ T$(kJ/mol). The nanohardness and Young's modulus of the MC and MN were much higher than the matrix, and the plastic deformation energy of interstitial phases was lower than the matrix. The precipitation of MC and MN is beneficial to the mechanical properties of coating.

1. Introduction

IN718 is a nickel-based superalloy widely used in high-temperature applications including turbine engines and power generation because of its excellent mechanical properties (yield strength up to 650–700 °C, impact strength and fracture toughness down to −40 °C) and corrosion resistance. The precipitation phases in the laser clad IN718 alloy coating include Laves, δ and MC. However, a small amount of MN [1,2] is found in the clad IN718 coating and weld. The brittle phase MC and MN [3,4] are formed during solidification of Ni-based superalloy to strengthen grain boundaries and improve the high-temperature mechanical properties. The previous literatures [5–10] have found that the MC was rich in Ti and Nb, and revealed that the MC was a eutectic product of L→(γ+NbC) at about 1245 °C. Hajmrle et al [6] had identified the chemical composition of a MN-type phase precipitated at about 1265 °C in heat-treated IN718 as 61Nb–18Ti–17Fe–3Ni–1Cr (wt%). The investigation on precipitation forms and the mechanical properties of MC and MN in the laser clad IN718 alloy coating is seldom reported. This paper not only investigates the chemical composition, precipitation forms and formation of Gibbs free energies of the MC and MN, and also measures the hardness and deformation energy of the MC and MN.

2. Experimental

The coatings were prepared with a 3.5 kW high power diode laser (Rofin DL-035Q) cladding system. The substrate used for the laser cladding is 6 mm thick IN718 alloy plate. The dimension of IN718 alloy powder for laser cladding is about 150 μm. Pure argon was used to prevent the molten pool from oxidation and contamination, and deliver the alloying powder to the molten pool. The clad coating was fabricated with different scanning speeds and the processing parameters were listed in Table 1. The energy distribution of the slow axis and fast axis is Gaussian distribution and top-hat distribution, respectively. The laser cladding processes along the fast axis. The energy density for the fabrication is about 182 W/mm^2. The chemical composition of the clad coating was 19.20 Cr, 18.1 Fe, 4.92 Nb, 0.54 Al, 0.97 Ti, 3.19 Mo, 0.20 Si, 0.04 Mn, 0.09 C, 0.11 N, and balance Ni in weight percent.

The microstructure of the coatings was observed with JSM-7600F field emission SEM equipped with EDS after etching with a Kalling's reagent (20 ml HCl, 20 ml C_2H_5OH and 1 g $CuCl_2$). The

* Corresponding author. Tel.: +86 21 54748940/8018; fax: +86 21 34203024.
E-mail address: lizg@sjtu.edu.cn (Z. Li).

0030-3992/$ - see front matter Crown Copyright © 2013 Published by Elsevier Ltd. All rights reserved.
http://dx.doi.org/10.1016/j.optlastec.2013.03.023

Table 1
Processing parameters for laser cladding.

Laser power (W)	1200
Scanning speed (mm/s)	8–50
Powder feed rate (g/min)	18
Shield gas flow (l/min)	15
Laterally shield gas flow (l/min)	8

chemical composition of precipitation phases was investigated by EDS and SPME. The cladded coating was pelt off the substrate and electrolyzed for SPME in the electrolyte solution of 7.5% KCl+0.5% citric acid diluted with distilled water at the temperature about −20 °C. The concentration of each element of the extractant is determined by inductively coupled plasma (ICP). The crystal structure and lattice constants of MC and MN were characterized by JSM-2100F field emission TEM. Vickers hardness of the coatings was measured on HVS-10 Vickers hardness tester at a load of 4.9 N for 15 s. The nanohardness and Young's modulus of the precipitation phases were investigated by nanoindentation with CMS 06-0140 nanoindentor. In the nanoindentation test, 3 locations of each phase were chosen. For each location, fifteen indentations were conducted in a 3×5 array with constant intervals. The applied load increased linearly to the peak load 5 mN in 30 s during the loading stage, and then the load was released in 30 s.

The nanohardness and Young's modulus of the materials can be derived through analysis of the loading–displacement data during the loading–unloading nanoindentation cycle using the method of Oliver and Pharr [11,12]. The nanohardness is given by Eq. (1) as:

$$H = \frac{F_{\max}}{A_c} \tag{1}$$

where, $F_{\max}$ is the maximum applied load and A_c is the area function of contact depth h_c.

Similarly, using the method of Oliver and Pharr, the calculation of elastic modulus of the material E_s is given by following Eqs. as:

$$E_r = \frac{1}{2}\sqrt{\frac{\pi}{A_c(h_c)}}\frac{dF}{dh} \tag{2}$$

$$\frac{1}{E_r} = \frac{1-\nu_s^2}{E_s} + \frac{1-\nu_i^2}{E_i} \tag{3}$$

where, E_s and ν_s are Young's modulus and Poisson's ratio of the specimen material, and E_i and ν_i are Young's modulus and Poisson's ratio of the indenter material, respectively. E_r is the effective Young's modulus of the contact pair indenter–specimen, E_r is obtained by nanoindentation. For the diamond indenter, E_i and ν_i are taken as 1141 GPa and 0.07, respectively.

3. Results and discussion

3.1. Microstructure

Fig. 1 depicts a typical cross section of single laser track obtained with the scanning speed of 8 mm/s. Good metallurgical bonding exists between the laser clad IN718 coating and the substrate. A large dilution region is formed under the high energy density, while the chemical composition of the coating is basically steady due to the similar chemical composition of the powder and the substrate. Fig. 2 shows the microstructure of the laser clad IN718 coatings fabricated with different scanning speeds. As shown in Fig. 2, the tetragonal and the insular precipitation phases appear in the coatings. The white dendritic Laves phase is refined and its concentration is decreased, and the concentration of the tetragonal and the insular phases increase slightly with increasing the scanning speed.

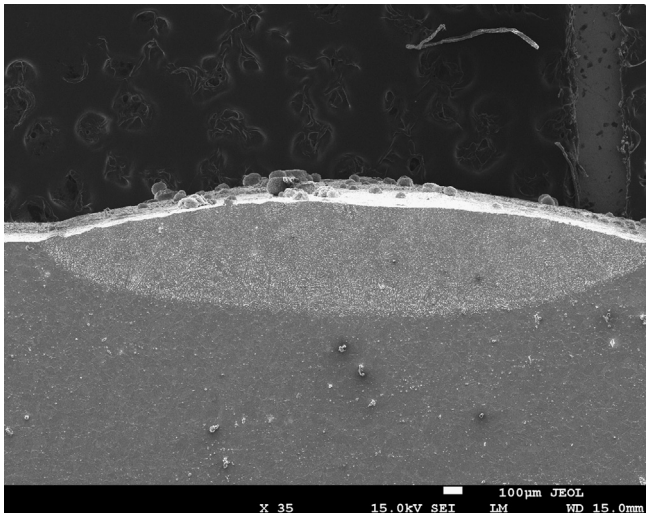

Fig. 1. Cross section of the cladded coating with scanning speed of 8 mm/s.

The white dendritic precipitation is Laves, the insular phase is MC-type carbide and the tetragonal phase is MN-type nitride [13,14]. The morphology of MC and MN varies from dendritic to petaline, and then tetragonal with increasing solidification rate. The grain growth rate is dependent on the difference between the atom deposition rate of solution atom depositing on the solid–liquid interface and the withdrawal rate of atoms escaping from the growth steps to the liquid alloy. The grain growth is dominated by the latent heat of fusion of the alloy, and the higher melting entropy is inclined to form finer and more homogeneous microstructure. Nevertheless, the supercooling of the molten pool increases with increasing the scanning speed and the cooling rate, and the large supercooling promotes the atom interface coarsening and forms the insular and/or tetragonal phases.

3.2. Precipitation form of phase

The EDS analysis was carried out to investigate the chemical composition of the MC and MN, as shown in Fig. 3 and Table 2. The results reveal that the tetragonal phase is rich in N, Ti and Nb, while the insular phase is rich in C, Ti and Nb. The precipitation phases contain large amounts of strong interstitial phase formation alloying elements (Nb and Ti), but without weak interstitial phase formation alloying elements (Fe and Ni) [15,16]. The concentrations of Ti and Nb in insular phase are (6.2–9) times and (16.7–18.4) times higher than the nominal concentration, respectively. The concentrations of Ti and Nb in tetragonal phase are (72–80) times and (2.8–4.5) times higher than the nominal concentration, respectively.

The forms of MC and MN are defined as $(Nb_\alpha Ti_{(1-\alpha)})C_\beta$ and $(Nb_x Ti_{(1-x)})N_y$ [17], α and x are the Nb atomic numbers, β and y are the non-metal atomic numbers in the sublattices of (NbTi)C and (NbTi)N, respectively. The calculational results according to Avogadro's principle show that $\alpha \approx 0.12$, $\beta \approx 1.5$, $x \approx 0.88$, and $y \approx 1.5$, respectively. However, the C concentration cannot be determined accurately by EDS. SPME for concentration of alloying elements in MC and MN is carried out. The coating mass for SPME is 12.31 g, and reclaimed mass of each element of MC and MN in the coating is presented in Table 3. The determination results of SPME agree well with the above calculation results when measurement error about 8% was taken into account. The measurement error is taken on the basis of the mass difference of each element between clad coating and the electrolyte solution. It is indicated that the formation of MC and MN is $(Nb_{0.12}Ti_{0.88})C_{1.5}$ and $(Nb_{0.88}Ti_{0.12})N_{1.5}$, respectively.